# Scattering of 217-Mev Positive Pions on Hydrogen*†

HORACE D. TAFT
*Department of Physics and The Enrico Fermi Institute for Nuclear Studies, The University of Chicago, Chicago, Illinois*

(Received September 2, 1955)

The total and differential cross section for the scattering of 217-Mev positive pions on hydrogen has been measured in nuclear emulsions. The total cross section, excepting Coulomb scattering, was found to be (151.0±18.2) mb. The angular distribution in the center of mass was fitted by $d\sigma/d\Omega=(5.22\pm1.42)+(7.53\pm2.57)\cos\chi+(20.36\pm4.61)\cos^2\chi$ mb/steradian, assuming $S$ and $P$ waves only. A phase shift analysis was carried out using the method of maximum likelihood. The phase-shift solution in agreement with the requirements of causality and corresponding to the preferred solution of de Hoffman *et al.* was $\alpha_3=-22.5°\pm5.8°$, $\alpha_{33}=114.0°\pm7.4°$, and $\alpha_{31}=-11.6°\pm9.7°$. The angular distribution showed strong forward scattering and a perference for positive Coulomb interference, in agreement with the hypothesis of a resonance in the state with angular momentum $\frac{3}{2}$ and isotopic spin $\frac{3}{2}$.

## INTRODUCTION

WITHIN the last year extensive analyses of pion-proton scattering data have been made by several authors[1–3] in the energy region between 120 Mev and 217 Mev. These analyses showed that the data were entirely consistent with the hypothesis of charge independence and with the assumption that only $S$ and $P$ waves contributed appreciably to the scattering at these energies. In particular, the analysis of de Hoffman *et al.*[2] resulted in a preferred solution indicating the presence of a resonance in the state with angular momentum $\frac{3}{2}$ and isotopic spin $\frac{3}{2}$ at an energy of approximately 197 Mev. The analysis made by these authors also indicated that as long as higher waves were negligible, the other two phase shifts which enter into $\pi^+$-proton scattering would be fairly small and negative in the energy region just above the resonance. The assumption of such a resonance, which was first proposed by Brueckner,[4] has recently been reinforced by the theoretical investigations of Chew and Low[5] and by the dispersion relations derived by Goldberger *et al.*[6] from the requirements of causality. It was therefore of considerable interest to examine $\pi^+$-proton scattering just above 200 Mev in order to compare the results with the following predictions of the proposed phase shift solution. The total cross section would drop rapidly with increasing energy from its value of about 200 mb measured just below 200 Mev. The angular distribution of the scattering would shift from backward to forward in passing through the resonance, since the amplitude of the scattered $P$ wave would change sign relative to the $S$-wave amplitude. The Coulomb interference would shift from negative to positive as the sign of the dominant $P$-wave amplitude changed. Finally, it was of interest to determine how large a contribution to the scattering cross section might be made by $D$ waves at these energies.

Due to the low fluxes of positive pions of energies greater than 150 Mev available from conventional synchrocyclotrons, several attempts have been made[7,8] to utilize nuclear track emulsions as well as cloud chambers[9] as tools for examining the angular distribution of $\pi^+$-proton scattering at high energies. More recently, by using heavy elements as targets in the internal circulating proton beam, both the Carnegie Tech group[10] and the Chicago group[11] have been able to extract sufficiently high fluxes of $\pi^+$ to perform counter measurements of angular distributions in the region between 150 Mev and 190 Mev. In addition, total cross sections above 150 Mev have been measured by the Carnegie Tech group[12] and by Yuan and Lindenbaum at Brookhaven.[13] The technique of exposing nuclear track emulsions inside the vacuum tank of a synchrocyclotron to obtain high-energy $\pi^+$ was utilized by Homa *et al.*[7] and has been attempted both at Carnegie Tech by Grandey and Clark and at Chicago by the present author. However, the very great shielding problems encountered in these attempts have made it seem preferable to work with $\pi^+$ beams outside the machine, even at the expense of very large reductions in flux. Since the flux of $\pi^+$ obtained in the present

* Work supported in part by the U. S. Atomic Energy Commission and the Office of Naval Research.

† Based on a thesis submitted to the Faculty of the Department of Physics, the University of Chicago, in partial fulfillment of the requirements for the Ph.D. degree.

[1] Fermi, Metropolis, and Alei, Phys. Rev. **95**, 1581 (1954).
[2] De Hoffman, Metropolis, Alei, and Bethe, Phys. Rev. **95**, 1586 (1954).
[3] R. L. Martin, Phys. Rev. **95**, 1606 (1954).
[4] K. A. Brueckner, Phys. Rev. **87**, 1026 (1952).
[5] G. F. Chew, Proceedings of the Fifth Annual Rochester Conference on High-Energy Physics (Interscience Publishers, Inc., New York, 1955).
[6] Goldberger, Miyazawa, and Oehme, Phys. Rev. **99**, 986 (1955).
[7] Homa, Goldhaber, and Lederman, Phys. Rev. **93**, 554 (1954).
[8] R. L. Grandey and A. F. Clark, Phys. Rev. **94**, 766 (1954).
[9] Fowler, Lea, Shephard, Shutt, Thorndike, and Whitemore, Phys. Rev. **92**, 832 (1953).
[10] Feiner, Ashkin, Blaser, and Stern, Phys. Rev. **98**, 239(A) (1955).
[11] M. Glicksman and H. L. Anderson, Phys. Rev. **100**, 268 (1955).
[12] Ashkin, Blaser, Feiner, Gorman, and Stern (to be published).
[13] L. C. Yuan and S. J. Lindenbaum, Proceedings of the Fifth Annual Rochester Conference on High-Energy Physics (Interscience Publishers, Inc., New York, 1955).

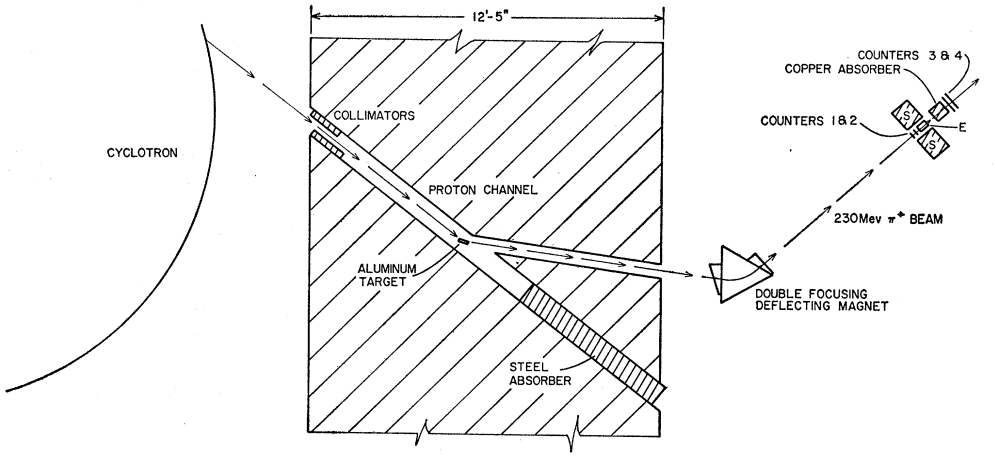


FIG. 1. Experimental arrangement. The emulsion stack $E$ and the shielding $S$ were not present while the range curve was taken.

experiment was extremely low, nuclear track emulsions were used in order to obtain a large number of scatterings in a reasonable running time and to obtain a high degree of discrimination against background events.

## PRODUCTION OF THE BEAM

Positive meson beams of energies greater than 200 Mev may be produced with the Chicago synchrocyclotron by producing the mesons outisde of the magnetic field at a target placed in an external proton beam and analyzing the mesons coming off in the forward direction. It was found that with all obstructions sufficiently retracted from the inside of the machine, about two percent of the internal circulating proton beam possessed small enough radial oscillations to pass through all coupling resonances and to escape from the machine with a uniform distribution of azimuthal angle. A small fraction of this spill-out beam possessed the proper azimuth to enter the proton channel in the shield wall, as shown in Fig. 1. The flux of protons measured at the entrance of this channel under normal operating conditions was approximately $10^7$ per cm$^2$ per second. This proton beam was quite parallel horizontally with a vertical height of about 1.5 in. The measured energy was $463\pm5$ Mev.

An aluminum target 4 inches long, 2 inches high, and 1 inch wide was placed at the intersection of the proton channel with a meson channel near the center of the shield wall as shown in Fig. 1. This target was oriented in such a way as to optimize the meson flux while presenting a width of no more than 2 inches to the analyzing magnet, in order to achieve the desired energy resolution of two percent. After passing through the target, the proton beam was stopped by more than 6 foot of steel, which was sufficient to reduce the neutron background in the experimental area to a level at which emulsion could be used. The entrance to the proton channel was collimated such that only the section of the channel filled by the target was irradiated.

## ENERGY ANALYSIS OF THE BEAM

In order to select pions of the proper momentum and to collect a large enough flux for experimental purposes, a 25° double-focusing wedge magnet was constructed from a 60° pair-spectrometer magnet by adding sections to the pole faces as indicated in Fig. 1. The double-focusing conditions were calculated from the equations of Camac,[14] and the calculated energy resolution across a 2-inch band at the focus was $\pm2$ percent, which was considered adequate for this experiment. Since this energy resolution depended strongly on the apparent size of the target, a helium-filled polyethylene tube was placed along the entire meson orbit to reduce multiple scattering and thus to approach the calculated energy resolution as closely as possible.

Since the proton flux in the accepted momentum range was approximately 40 times the pion flux, a counter system sensitive only to protons of $60\pm13.5$ Mev was used to adjust the magnet current to select a momentum of approximately 341 Mev/$c$, corresponding to a pion energy of 229 Mev. With this magnet current a range curve was taken of the pions in the beam, using the counter geometry shown in Fig. 1. The two leading counters were 2-inch by 2-inch plastic scintillators $\frac{1}{8}$-inch thick. The following two counters were 8-inch diameter liquid scintillators described by Anderson *et al.*[15] The range curve obtained, including correction for counter thicknesses, is shown in Fig. 2. This curve is made up of counts taken both before and after the exposure to check that operating conditions did not change during the experiment.

The integral range curve was analyzed as indicated in Fig. 2 to determine the mean measured range of the pion beam. The less steep portion of the curve at absorber thicknesses greater than 130 g/cm$^2$ of copper was assumed to be due to muons and positrons, and when extrapolated back to zero absorber thickness,

[14] M. Camac, Rev. Sci. Instr. **22**, 197 (1951).
[15] Anderson, Fermi, Martin, and Nagle, Phys. Rev. **91**, 155 (1953).

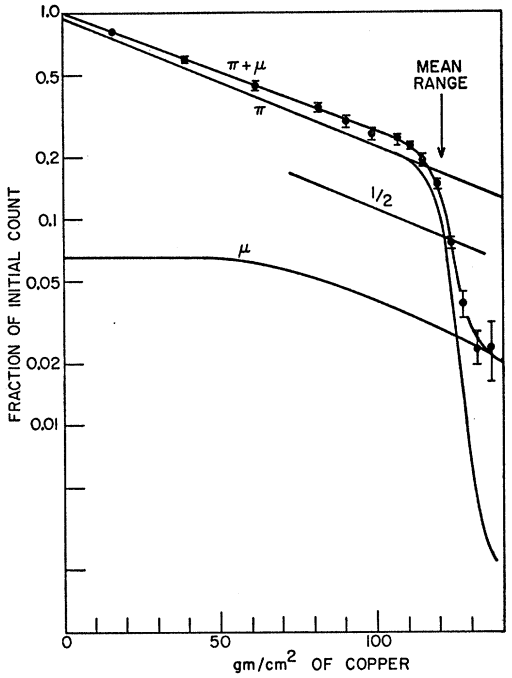


FIG. 2. Range curve. The mean measured range before correcting for multiple scattering was 121.0 g/cm² of copper.

indicated a total contamination of 6.5 percent as explained in the following section. After subtracting out this contamination, the mean measured range was found to be 121.0 g/cm² of copper. After correcting for multiple scattering and statistical straggling as explained in the Appendix, the true range was determined to be 124.4±3.4 g/cm² of copper. Using 139.6 Mev for the pion mass[16] and 6.721 for the proton to pion mass ratio, Aron's range-energy tables[17] give 231±5 Mev as the energy of the pion beam.

## CONTAMINATION

The $\mu$ meson and positron contamination in the beam was estimated by dividing the sources of contamination into three classes and treating them separately as follows:

### (A) Positrons and μ Mesons Produced before the Analyzing Magnet

Only pions of energies greater than 224 Mev could have produced muons of the proper momentum, and since the muon energy spectrum for a given pion energy is flat and extends over a region about 150 Mev wide, only a small fraction of these muons were accepted by the magnet. Further, very few pions of energy greater than 250 Mev could be produced. By using these considerations, an estimate was obtained of the contamination coming through the magnet of the order of 1 percent, which is not in disagreement with the more reliable estimate of 1.5 percent obtained from the range curve.

### (B) Pion Decays between the Magnet and the Counter Telescope

About 10 percent of the pions in the beam decayed between the magnet and the first counter, and since the angular dependence of these decays in the laboratory system was known, it was calculated that approximately 30 percent of the muons passed through the counter telescope. The energy spectrum of these muons was such that only 12.5 percent had ranges greater than 136 g/cm² of copper.

### (C) Pion Decays between the First and Last Counter

About 2 percent of the pions in the beam decayed between the first and last counter, but less than 10 percent of the muons from these decays reached an absorber thickness of 136 g/cm² of copper.

The total contamination from these three sources is plotted in Fig. 2.

The contamination in the emulsion was calculated from the above considerations to be 4.5 percent. In scanning, however, only tracks whose projected angles in the horizontal plane were within ±4° of the beam direction were accepted. Due to the vertical shrinkage of the emulsion during processing, the criterion set on the dip angle was less precise. Knowing the angular distribution of muons from pion decays, the approximate angular spread of the incident beam, and the multiple scattering to be expected in the 1 cm of emulsion preceding the scanning region, it was calculated that the muon and positron contamination in the scanning region was (3.5±2) percent. An addition of (3±1) percent was made to this figure due to cosmic-ray contamination in the emulsion. An unexposed control pellicle from the same package of emulsion was found to contain a flux of minimum tracks in the identical direction and solid angle accepted in the exposed pellicles corresponding to approximately 3 percent of the total pion flux obtained. The total nonpion contamination in the scanning region was therefore taken to be (6.5±2.3) percent.

A rough check on this number may be obtained by comparing the nonhydrogen interaction cross section of the present experiment with that of Morrish[18] at 217 Mev ($\pi^-$) and with that of Grandey and Clark[8] at 151 Mev ($\pi^+$). Assuming that this nonhydrogen interaction cross section is not strongly dependent on charge or on energy in this energy region, Morrish's results would lead to a contamination in the present experiment of (8.9±10) percent, while Grandey and

[16] K. M. Crowe and R. H. Phillips, Phys. Rev. **96**, 470 (1954).
[17] W. A. Aron, University of California Radiation Laboratory UCRL-1325, 1951 (unpublished).
[18] A. H. Morrish, Phys. Rev. **90**, 674 (1953).

Clark's results would give (4±7) percent. Neither of these figures is in disagreement with our accepted value.

## EXPOSURE

The experimental arrangement during the exposure is shown in Fig. 3. In order to insure that the recoil protons from a large fraction of pion-proton scatterings could be followed to the end of their range (as a check on the kinematics of the event), a stack of thirty-six 2-inch by 4-inch 1200 micron Ilford G-5 emulsion pellicles was placed in the beam preceded only by the monitoring counters. As a check on the counter range curve, another stack was placed in the beam, preceded by sufficient absorber so that positive pions of the proper energy would stop near the center of this stack. In order to avoid altering the characteristics of the beam during the slowing down process, both stacks were imbedded in cylinders of pseudite,[19] a material which closely duplicates the stopping power and scattering of emulsion.

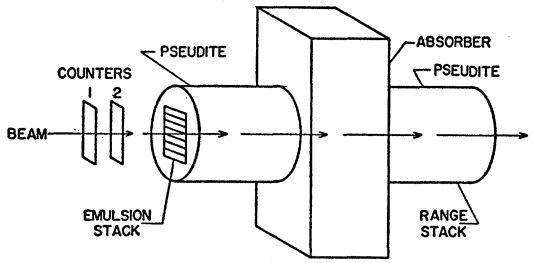


FIG. 3. Experimental arrangement during exposure. The absorber was 62.89 g/cm² of copper. The range stack consisted of four 2-inch by 4-inch Ilford G-special 1800 micron emulsion pellicles.

This arrangement was exposed to a total flux of 3600 $\pi^+$ per cm², obtained in 42 hours of running time. However, the central dozen, which comprised most of the plates scanned, was replaced by a fresh dozen midway in the exposure in order to reduce the background, and hence contained only half of this flux. The extremely low intensity, combined with the attenuation and scattering in the absorber, reduced the flux of pions in the range stack to a point where insufficient statistics could be obtained to give more than a rough check on the counter range curve. The agreement between the emulsion range curve and the counter range curve was satisfactory.

## SCANNING PROCEDURE

Because of the low flux, the technique of scanning along the track was employed. This method is faster than area scanning for very low fluxes and has the advantage that the scanning efficiency is very close to 100 percent. Scanners were instructed to find minimum ionizing tracks within ±3° of the beam direction, which was determined for each pellicle to ±1°, starting at a line 1 cm from the leading edge of the pellicle. By this point the high flux of 60-Mev protons accepted by the magnet was almost entirely stopped. Each track was followed until it either left the surface of the emulsion or traveled 3 cm. When a track caused a star or was deflected by >3°, the event was recorded and a new track was located at the starting line. Each track could be easily re-located and rescanned. In rescanning over 150 such tracks ending in recognizable events, no scanning errors or switching from one track to another were detected. Since such interchanging of tracks should be the largest factor in scanning inefficiency, the scanning efficiency was taken to be 100 percent to within the accuracy of the experiment. As a further check on scanning efficiency, the distribution in azimuthal angle of the events is given in Fig. 4. This distribution is constant to within statistical errors.

The low flux and reasonable background in the plates tended to reduce possible confusion of tracks and allowed scanning rates of 30 to 40 cm per hour. A small angle cutoff of 7.4° (10° in the center of mass) was set for hydrogen events due to the difficulty of positive identification at smaller angles, but no large angle cutoff was necessary since scatterings close to 180° are as easily detected by track scanning as are those at other angles.

## IDENTIFICATION OF EVENTS

All events initiated by a minimum ionizing track and consisting of a forward scattered track of greater than twice minimum and a light scattered track on the opposite side of the incident direction were measured. The criterion of coplanarity was applied by computing the volume of the parallelepiped generated by the three unit vectors involved. This volume may be written in the form

$$F=\cos\beta_0\cos\beta_\pi\cos\beta_p[\sin\alpha_\pi\tan\beta_p-\sin\alpha_p\tan\beta_\pi+\sin(\alpha_p-\alpha_\pi)\tan\beta_0], \quad (1)$$

where $\beta_0$, $\beta_\pi$, and $\beta_p$ are the dip angles of the incoming pion, the scattered pion, and the recoil proton, respec-

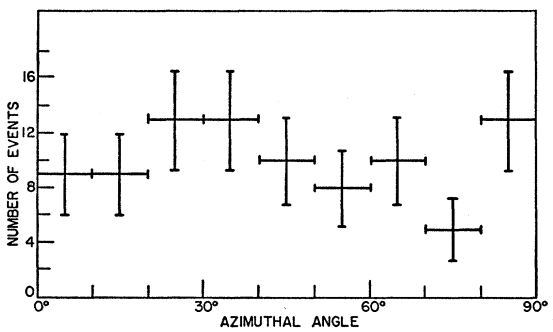


FIG. 4. A plot of the number of events *vs* the azimuthal angle.

[19] A. H. Rosenfeld, Phys. Rev. **96**, 139 (1954).

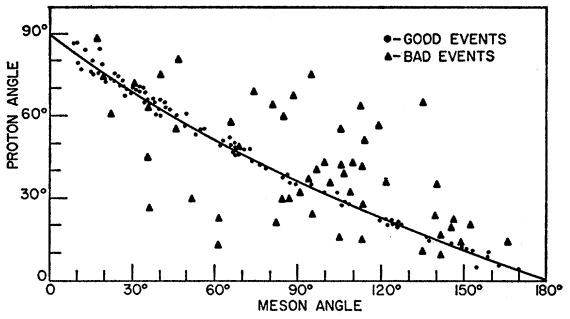


FIG. 5. Angular correlation of events. The curve is for 220-Mev $\pi$ mesons. The bad events within 5° of the curve have been ruled out on the basis of coplanarity or range.

tively, relative to the plane of the emulsion, and $\alpha_\pi$ and $\alpha_p$ are the angles projected in the plane of the emulsion between the scattered pion and proton tracks and the direction of the incoming pion track. The maximum value of $F$ is 1 and $F=0$ corresponds to perfect coplanarity. The empirical standard deviation on $F$ for all scatterings greater than 30° in the laboratory system was found to be $\langle F\rangle_{rms}=0.02$, in good agreement with work of Orear.[20] For scatterings less than 30°, the standard deviation was about twice this value, due to the multiple scattering of the low-energy recoil proton, but the range of the recoil proton provided a more stringent check in all these cases.

Measurement of the scattering angles provided a further check on the identification of pion-proton events since the change in the required angular correlation due to changes in energy over the region involved is extremely small. The events found are plotted in Fig. 5 together with the kinematic curve for 220-Mev pions on protons.[21] The perpendicular distance to the kinematic curve from the experimental point was used as a measure of the deviation of the event from perfect correlation and is denoted by $\Delta\theta$. The empirical standard deviation on $\Delta\theta$ was found to be $\langle\Delta\theta\rangle_{rms}=2°$ for scatterings of greater than 30° and 3° for smaller angle scatterings. A plot of the number of events per unit area in $F$ and $\Delta\theta$ *vs* the quantity $[(F)^2+(\Delta\theta)^2]^{\frac{1}{2}}$ is given in Fig. 6, where $F$ and $\Delta\theta$ are in units of their standard deviations. An estimate of the background subtraction to be made for nonhydrogen events which appeared to be elastic scatterings was obtained by making the crude assumption that such events were uniformly distributed on a plot of $F$ *vs* $\Delta\theta$ and by extrapolating the background into the acceptable region. This procedure, although very approximate, was adequate because of the smallness of the background subtraction. A comparison of the area under the curve for hydrogen events with the area under the extrapolated background curve in Fig. 6 gave a background subtraction of 3 events out of a total of 91, with an estimated error of ±2 events. One such event was found by noting a discrepancy in the range of the recoil proton, as discussed in the following section.

[20] J. Orear, Phys. Rev. **92**, 156 (1953).
[21] H. L. Anderson and D. G. Wilson (unpublished tables).

## ENERGY DISTRIBUTION OF EVENTS

The energy distribution of the events was determined by two methods. The first method consisted in determining the incident pion energy by measuring the ranges of the recoil protons from 47 apparent pion-proton events. Of these events, 39 had values of the coplanarity parameter $F$ and of the angular correlation parameter $\Delta\theta$ within the accepted limit of 2.5 standard deviations. Only one of these acceptable events had a recoil proton with a range inconsistent with the range to be expected from an elastic collision between a proton and a pion whose energy was determined from the counter range curve plus the known energy loss in emulsion. Of the remaining 8 events which were noncoplanar or had scattering angles differing from the kinematic curve by more than 2.5 standard deviations, all had inconsistent recoil proton ranges. The energy distribution of the events measured by this method had a mean energy of 215.4 Mev and a half-width at half-maximum of about 10 Mev.

The energy distribution of all of the events was also determined by assuming an incident pion energy of 231 Mev, as given by the counter range curve, and by taking into account the energy loss of the pion in the emulsion preceding each event. This energy distribution is shown in Fig. 7. The mean energy of this distribution was computed to be 216.5 Mev with a half-width at half-maximum of about 6 Mev, in good agreement with the distribution obtained from recoil proton ranges.

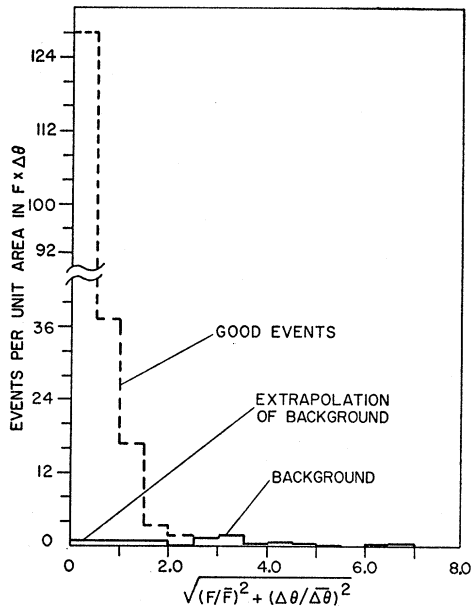


FIG. 6. A plot of the number of events per unit area in $F$ and $\Delta\theta$ *vs* $[(F)^2+(\Delta\theta)^2]^{\frac{1}{2}}$ in units of standard deviations. The background subtraction was 3±2 events.

The latter distribution, however, was affected by errors in the measurement of scattering angles as well as by uncertainties in the vertical shrinkage factor of the emulsion.

By using the distribution of Fig. 7, it was calculated that the correction to the total cross section due to the energy spread of the events was negligible, assuming a reasonable energy dependence of the cross section in this energy region. A similar calculation for the dominant phase shift $\alpha_{33}$ also gave a negligible correction. However, the estimated uncertainty of $\pm 2$ Mev in the mean energy of the incident pion beam was equivalent to an uncertainty of $\mp 2$ percent in the total cross section, which was not entirely negligible.

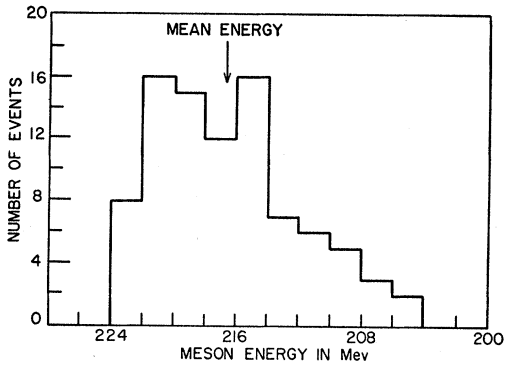


FIG. 7. The energy distribution of the events based on an incident pion energy of 231 Mev.

## RESULTS

A total of 11 787 tracks were followed for a total path length of 20 545 cm. Subtracting muon and positron contamination, the effective path length scanned was 19 210 cm$\pm$2.3 percent. In this path length, 620 nonhydrogen stars, 640 recoilless scatterings of greater than 3°, and 90 hydrogen scatterings, with a background subtraction of $2\pm 2$, were found. The corresponding mean free paths in emulsion are

| Interaction | Mean free path |
|---|---|
| Star | 31.0$\pm$1.4 cm |
| Recoilless scattering>3° | 30.0$\pm$1.4 cm |
| Hydrogen scattering>7.4° | 218.3$\pm$25.1 cm |

In order to compute the hydrogen scattering cross section, the number of protons per cm$^3$ was obtained from recent data on the composition of Ilford G-5 emulsion supplied by Waller[22] of Ilford Ltd. These data indicate that at a relative humidity of 40 percent $\pm$15 percent at which the emulsion was exposed, the hydrogen density of the emulsion was $0.0508\pm 0.0019$ g/cm$^3$, corresponding to $3.035\times 10^{22}$ protons per cm$^3$. Using this result, the total cross section for pion-proton scatterings at angles greater than 10° in the center-of-mass system was

$$\sigma_{\text{total}}=\frac{[90-(2\pm 2)]\pm 9.5}{[(3.035\pm 0.114)\times 10^{22}\ \text{cm}^{-3}][19\,210\pm 430\ \text{cm}]}$$

$$=150.9\pm 17.5\ \text{mb}.$$

TABLE I. Center-of-mass scattering angles for the 90 acceptable events.

| Event | Angle | Event | Angle | Event | Angle |
|---|---|---|---|---|---|
| 1 | 12.6° | 31 | 45.1° | 61 | 89.8° |
| 2 | 12.7° | 32 | 46.3° | 62 | 95.8° |
| 3 | 13.6° | 33 | 47.4° | 63 | 101.6° |
| 4 | 14.2° | 34 | 48.8° | 64 | 102.4° |
| 5 | 15.8° | 35 | 50.1° | 65 | 104.2° |
| 6 | 16.3° | 36 | 50.8° | 66 | 110.4° |
| 7 | 19.8° | 37 | 51.2° | 67 | 115.9° |
| 8 | 20.1° | 38 | 52.0° | 68 | 118.6° |
| 9 | 20.6° | 39 | 52.1° | 69 | 121.0° |
| 10 | 22.3° | 40 | 53.4° | 70 | 121.6° |
| 11 | 22.3° | 41 | 53.6° | 71 | 122.6° |
| 12 | 23.9° | 42 | 54.0° | 72 | 133.8° |
| 13 | 25.1° | 43 | 55.2° | 73 | 135.4° |
| 14 | 26.7° | 44 | 59.4° | 74 | 136.4° |
| 15 | 30.6° | 45 | 61.7° | 75 | 137.8° |
| 16 | 31.2° | 46 | 63.2° | 76 | 138.6° |
| 17 | 32.4° | 47 | 67.7° | 77 | 139.8° |
| 18 | 32.4° | 48 | 68.7° | 78 | 139.9° |
| 19 | 32.7° | 49 | 68.8° | 79 | 140.2° |
| 20 | 34.2° | 50 | 77.8° | 80 | 140.4° |
| 21 | 36.4° | 51 | 77.8° | 81 | 148.9° |
| 22 | 36.4° | 52 | 79.0° | 82 | 149.1° |
| 23 | 36.7° | 53 | 81.6° | 83 | 155.3° |
| 24 | 38.4° | 54 | 82.1° | 84 | 157.4° |
| 25 | 38.9° | 55 | 82.4° | 85 | 158.1° |
| 26 | 39.2° | 56 | 82.7° | 86 | 160.2° |
| 27 | 39.9° | 57 | 83.8° | 87 | 164.4° |
| 28 | 40.3° | 58 | 83.8° | 88 | 164.8° |
| 29 | 41.0° | 59 | 86.6° | 89 | 166.9° |
| 30 | 44.6° | 60 | 87.6° | 90 | 172.7° |

In determining the angular distribution, the scattering angle for each scattering of greater than 30° was assumed to be given by the point on the kinematic curve of Fig. 5 nearest to the actual measured angles. For scatterings of less than 30°, the measured deflection of the pion track was considered a more reliable estimate. The center-of-mass angles for the 90 acceptable events are given in Table I.

## PHASE-SHIFT ANALYSIS

In order to interpret the total cross section and angular distribution obtained in this experiment and to compare the results with theoretical predictions, a phase-shift analysis of the data was performed under the assumption that no states with orbital angular momentum greater than $2\hbar$ contribute appreciably to the scattering. For convenience in calculating, we define a quantity

$$s(x)=k^2\frac{d\sigma}{d\Omega}(x), \tag{2}$$

where $x$ is the cosine of the scattering angle, $k$ is the wave number of the pion and $(d\sigma/d\Omega)(x)$ is the differential cross section in cm$^2$ per steradian at the angle $\cos^{-1}x$ (all quantities in the center-of-mass system). The formulas used to write $s(x)$ in terms of the phase

[22] C. Waller (private communication to Dr. A. H. Rosenfeld).

shifts are based on those derived by Solmitz,[23] but differ in two respects. Terms were added to include the possible contribution of $D$ waves to the cross section, and Coulomb phase factors were taken into account up to and including terms of first order in the quantity

$$n=(e^2/\hbar c)\times(1/\beta_\pi), \tag{3}$$

where $\beta_\pi=(1/c)\times$velocity of the pion in the laboratory system. With these modifications, the differential cross section may be written

$$k^2\frac{d\sigma}{d\Omega}(x)=s(x)=|kf^{(nf)}(x)|^2+|kf^{(f)}(x)|^2, \tag{4}$$

where

$$kf^{(nf)}(x)=\frac{1}{2i}\left\{e_0+(1+2in)(2e_1^{+}+e_1^{-})x+(1+3in)(3e_2^{+}+2e_2^{-})\frac{3x^2-1}{2}\right\}+\left(-\frac{n}{1-x}+a\right)\left(1-in\ln\frac{1-x}{2}\right), \tag{5}$$

TABLE II. Results of the phase-shift analysis.

| Solution | Initial values | Final values | $w$[a] |
|---|---|---|---|
| | Case 1: $S$ and $P$ waves only | | |
| I | $t=0.0$<br>$\alpha_3=-22.5°$<br>$\alpha_{33}=-67.5°$<br>$\alpha_{31}=-5.6°$ | 0.01<br>$-22.5°$<br>$-66.0°$<br>$-11.6°$ | $-0.0405$ |
| II | $t$ not varied<br>$\alpha_3=-22.5°$<br>$\alpha_{33}=-39.4°$<br>$\alpha_{31}=-90.0°$ | $-22.5°$<br>$-36.6°$<br>$+89.2°$ | $-0.0405$ |
| III | $t=0.0$<br>$\alpha_3=+22.5°$<br>$\alpha_{33}=+67.4°$<br>$\alpha_{31}=+5.6°$ | $-0.01$<br>$+24.9°$<br>$+67.4°$<br>$+14.3°$ | $-0.4394$ |
| IV | $t=0.0$<br>$\alpha_3=+78.8°$<br>$\alpha_{33}=-33.8°$<br>$\alpha_{31}=-33.8°$ | $-0.05$<br>$+76.1°$<br>$-35.3°$<br>$-34.7°$ | $-0.2244$ |
| | Case 2: $S$, $P$, and $D$ waves | | |
| I | $t=0.0$<br>$\alpha_3=-22.5°$<br>$\alpha_{33}=-66.1°$<br>$\alpha_{31}=-11.6°$<br>$\delta_{35}=0.0°$<br>$\delta_{33}=0.0°$ | 0.0<br>$-22.4°$<br>$-66.0°$<br>$-11.7°$<br>$+0.03°$<br>$+0.05°$ | $-0.0402$ |
| I | $t$ not varied<br>$\alpha_3=-24.6°$<br>$\alpha_{33}=-60.7°$<br>$\alpha_{31}=-20.5°$<br>$\delta_{35}=+11.3°$<br>$\delta_{33}=+11.3°$ | $-22.7°$<br>$-65.7°$<br>$-12.6°$<br>$+0.19°$<br>$+0.75°$ | $-0.0424$ |

[a] The quantity $w$ is given to within an arbitrary constant term.

[23] F. Solmitz, Phys. Rev. 94, 1799 (1954).

and

$$kf^{(f)}(x)=-(1-x^2)^{\frac{1}{2}}\left[\frac{1}{2i}\{(1+2in)(e_1^{+}-e_1^{-})+(1+3in)(e_2^{+}-e_2^{-})3x\}-\frac{b}{1-x}\right], \tag{6}$$

where

$$a=n\frac{\beta_p'}{1+\beta_\pi'\beta_p'}\left[\beta_\pi'+\frac{2\mu_p-1}{2}\beta_p'\right],$$

and

$$b=n\frac{\beta_p'}{1+\beta_\pi'\beta_p'}\left[\mu_p\beta_\pi'+\frac{2\mu_p-1}{2}\beta_p'\right],$$

where $\beta_\pi'=(1/c)\times$velocity of pion in the center-of-mass system, $\beta_p'=(1/c)\times$velocity of proton in the center-of-mass system, $\mu_p=$magnetic moment of the proton in nuclear magnetons$=2.7896$, and $e_l^{\pm}=\exp[2i\alpha_{3,2l\pm1}]-1$, where $\alpha_{3,2l\pm1}$ is the phase shift of the scattered wave with orbital angular momentum $l\hbar$ and total angular momentum $j\hbar=(l\pm\frac{1}{2})\hbar$. The $S$-wave phase shift is written $\alpha_3$, and to avoid an ambiguity when $l=2$, we write $D$-wave phase shifts as $\delta$'s. The quantities $a$ and $b$ are included in the treatment for completeness, although they are rather small at these energies. $f^{(nf)}(x)$ and $f^{(f)}(x)$ are the nonspin-flip and spin-flip scattering amplitudes, respectively.

The 90 events listed in Table I were analyzed using the method of maximum likelihood.[24] Writing the differential cross section as a function of a particular set of phase shifts $[\alpha]$ which determine the quantity $s(x;[\alpha])$ at all $x$, the average number of events (average understood to be over many identical experiments) in the angular interval $dx$ for one experiment is $Cs(x;[\alpha])\times dx$, where $C=2\pi N\lambda/k^2$, $N=$number of scattering centers per cm$^3$, and $\lambda=$path length scanned. The average total number of events for one experiment is then $\int_{x_{\min}}^{x_{\max}}Cs(x;[\alpha])dx$, where the limits of the integral correspond to the maximum and minimum angles detected. According to the Poisson distribution, the probability of finding no event in the angular interval $dx$ is $\exp[-Cs(x;[\alpha])dx]$ and the probability of finding just one event is $Cs(x;[\alpha])dx\exp[-Cs(x;[\alpha])dx]$. The probability of finding just $p$ events, one each at $\cos\chi_1=x_1$, $\cos\chi_2=x_2$, $\cdots\cos\chi_p=x_p$ in the intervals $dx_1$, $dx_2$, $\cdots dx_p$ is given by

$$\mathfrak{L}_p(x_1,x_2\cdots x_p;[\alpha]C)\prod_{i=1}^{p}dx_i=\exp\left[-\int_{x_{\min}}^{x_{\max}}Cs(x;[\alpha])dx\right]\prod_{i=1}^{p}Cs(x_i;[\alpha])dx_i. \tag{7}$$

The maximum likelihood method consists in maximizing

[24] For a more complete discussion of the application of this method to the analysis of experiments, see F. Solmitz, Revs. Modern Phys. (to be published).

the quantity

$$w=\ln\mathfrak{L}_p=\sum_{i=1}^{p}\ln Cs(x_i;[\alpha])-\int_{x_{\min}}^{x_{\max}}Cs(x;[\alpha])dx \quad (8)$$

as a function of the parameters $[\alpha]$. If one assumes that $C$ is a normally distributed quantity with a mean value $C_0$ and a standard deviation $\mu$, one may include the effect of this uncertainty by writing

$$w=\sum_{i=1}^{p}\ln(C_0+\mu t)s(x_i;[\alpha])-\int_{x_{\min}}^{x_{\max}}(C_0+\mu t)s(x;[\alpha])dx-\frac{t^2}{2}, \quad (9)$$

where $t$ is the number of standard deviations away from $C_0$ at which $w$ is computed, and we have dropped constant terms since only changes in $w$ are significant for the analysis.

The problem of maximizing $w$ by a systematic variation of the input parameters, i.e., the phase shifts and the deviation of $C$ from its mean measured value, was solved by means of an electronic computer.[25] According to the maximum-likelihood method, the best solution to the data is given by the particular set of parameters which maximizes $w$. Two procedures were used. In the first procedure, only $S$ and $P$ waves and the Coulomb terms were allowed to contribute, while $D$ waves were held at zero. In this way, four solutions were examined with the results shown in Table II. The first three of these are commonly known as the Fermi solution, denoted by I, the Yang solution, denoted by II, and the complex conjugate Fermi solution, denoted by III. These three solutions are all characterized by a small absolute magnitude of $\alpha_3$. Except for Coulomb effects, the magnitude of $\alpha_3$ for these three solutions would be identical, and all three solutions would give identical differential cross sections. The presence of Coulomb effects does not discriminate between the Fermi and Yang solutions, but does result in a lower value of $w$ for Solution III, the significance of which will be discussed below. The complex conjugate Yang solution was not examined because it yields a differential cross section indistinguishable from that of Solution III. Solution IV is of a different class of solutions with large $\alpha_3$. This solution gave a poorer fit to the data than did Solutions I and II, but cannot be entirely ruled out on the basis of the present data alone.

In the second procedure, all six parameters were varied, with the results shown in Table II. The outstanding feature of the results of this second procedure is that no significantly better fit to the data could be obtained by allowing $D$ waves to contribute, even when a relatively large amount of $D$ wave was inserted at the beginning of the hunting procedure. On the other hand, the errors on the $D$-wave phase shifts are quite large, as shown below, and greatly improved statistics would be required to establish reliable values for these phase shifts, even as to their sign.

[25] The maximizing procedure as well as the error analysis were developed by Dr. William C. Davidon, using the AVIDAC at the Argonne National Laboratory.

## ERROR ANALYSIS

In order to obtain an estimate of the errors on the phase shifts, we assume that in the region of a maximum the quantity $w$ depends quadratically on the deviations of the parameters (the phase shifts and the quantity $t$) from their best fit values. The actual dependence of $w$ on these deviations was then fitted to the assumed form

$$w=w_{\max}-\tfrac{1}{2}\sum_{i,j}G_{ij}\epsilon_i\epsilon_j, \quad (10)$$

where $w_{\max}$ is the maximum value of $w$ in this region, $\epsilon_i$ is the deviation of the $i$th parameter from its best fit value, and $G$ is a real, symmetric matrix with positive eigenvalues. The elements of $G$ were determined by using the AVIDAC and varying all pairs of parameters separately until $w$ was diminished by $\frac{1}{2}$ in each case. These variations were then averaged as described by Anderson *et al.*,[26] and the best fit elements of $G$ were determined. As pointed out by Anderson *et al.*,[26] $G$ is not affected to first order by a small displacement of the elliptical surface of constant $w$ in any direction. Since $e^{+w}$ is a measure of the relative probability of having obtained the experimental results given any particular set of parameters $[\alpha]$, the accuracy with which these parameters have been determined may be expressed by the error matrix $G^{-1}$ with the property

$$\langle\epsilon_i\epsilon_j\rangle_{Av}=\frac{\int\cdots\int\epsilon_i\epsilon_j e^w d\epsilon_1\cdots d\epsilon_m}{\int\cdots\int e^w d\epsilon_1\cdots d\epsilon_m}=(G^{-1})_{ij}. \quad (11)$$

TABLE III. The error matrices $G^{-1}$.[a]

| | Case 1: $S$ and $P$ waves | | | |
|---|---|---|---|---|
| | $t$ | $\alpha_3$ | $\alpha_{33}$ | $\alpha_{31}$ |
| $t$ | 7.921 | 3.079 | 8.056 | 3.581 |
| $\alpha_3$ | | 34.053 | 5.958 | −1.189 |
| $\alpha_{33}$ | | | 54.803 | 0.599 |
| $\alpha_{31}$ | | | | 93.882 |

| | Case 2: $S$, $P$, and $D$ waves | | | | | |
|---|---|---|---|---|---|---|
| | $t$ | $\alpha_3$ | $\alpha_{33}$ | $\alpha_{31}$ | $\delta_{35}$ | $\delta_{33}$ |
| $t$ | 7.930 | 2.952 | 8.372 | 2.922 | 0.293 | 1.017 |
| $\alpha_3$ | | 56.231 | −21.801 | 53.721 | −68.647 | 4.487 |
| $\alpha_{33}$ | | | 92.572 | −74.746 | 84.017 | 14.387 |
| $\alpha_{31}$ | | | | 244.303 | −165.797 | −32.637 |
| $\delta_{35}$ | | | | | 213.682 | −26.478 |
| $\delta_{33}$ | | | | | | 133.153 |

[a] The units are (degrees)$^2$. The quantity $t$, when multiplied by $(32/90)^2$, is in units of (number of standard deviations)$^2$.

[26] Anderson, Davidon, Glicksman, and Kruse, Phys. Rev. **100**, 279 (1955).

Thus the square roots of the diagonal elements of $G^{-1}$ give the standard deviations for each of the parameters, while the off-diagonal elements are the products of the correlation coefficients with the two corresponding standard deviations. The matrices $G^{-1}$ for error analyses both with and without $D$ waves are given in Table III.

There are several internal checks on the validity of this procedure for determining errors on the phase shifts. To check that $w$ was very nearly quadratic in the parameters near its maximum value, the AVIDAC was instructed during the hunting procedure before each new phase shift variation to guess what value of $w$ this new variation would give, based on the behavior of $w$ in the vicinity of the previous trial point and on the assumption that $w$ was quadratic. This guess invariably proved to be extremely accurate near the maximum. Secondly, a computation of the statistical error on the total cross section, using the statistical errors on the phase shifts as well as correlations between these phase shifts as determined from the above procedure, gives a result in very good agreement with the statistical error associated with 90 events. Finally, the fact that the square root of the diagonal element of $G^{-1}$ associated with the quantity $C$ is indeed 1.00 standard deviations is an indication of the validity of the assumptions involved in the error analysis. The following results were obtained for Solution I, the stated errors being statistical plus a 5 percent uncertainty in in the path length scanned.

*Case 1.*—$S$ and $P$ waves and $t$ ($t$ in units of standard deviations);

| $t$ | $\alpha_3$ | $\alpha_{33}$ | $\alpha_{31}$ |
|---|---|---|---|
| $0.01\pm1.00$ | $-22.5°\pm5.8°$ | $114.0°\pm7.4°$ | $-11.6°\pm9.7°$ |

*Case 2.*—$S$, $P$, and $D$ waves and $t$ ($t$ in units of standard deviations);

| $t$ | $\alpha_3$ | $\alpha_{33}$ | $\alpha_{31}$ |
|---|---|---|---|
| $0.00\pm1.00$ | $-22.4°\pm7.5°$ | $114.0°\pm9.6°$ | $-11.7°\pm15.6°$ |

| $\delta_{35}$ | $\delta_{33}$ |
|---|---|
| $0.03°\pm14.6°$ | $0.05°\pm22.5°$ |

The total cross section, excluding Coulomb scattering, from Solution I is $\sigma_{\text{total}}=151.0\pm18.2$ mb. From the Solution I phase shifts, assuming $S$ and $P$ waves only, the differential cross section is given by

$$d\sigma/d\Omega=(5.22\pm1.42)+(7.53\pm2.57)\cos\chi+(20.36\pm4.61)\cos^2\chi \text{ mb/steradian.}$$

TABLE IV. Experimental value of $(2k_b^2/k)D_+(k)$.

| Solution | $\sin2\alpha_3+2\sin2\alpha_{33}+\sin2\alpha_{31}+3\sin2\delta_{35}+2\sin2\delta_{33}$ |
|---|---|
| I ($S$ and $P$ waves only) | $-2.58\pm0.47$ |
| I ($S$, $P$, and $D$ waves and $C$) | $-2.59\pm0.97$ |
| II ($S$ and $P$ waves only) | $-2.59$ |
| III ($S$ and $P$ waves only) | $+2.66$ |
| IV ($S$ and $P$ waves only) | $-2.36$ |

## DISPERSION RELATIONS

Dispersion relations expressing the real parts of the forward scattering amplitudes in terms of integrals over the total interaction cross sections have been derived from the requirements of causality by Goldberger, Miyazawa, and Oehme[6] for the scattering of positive and negative pions on protons. These relations may be written

$$D_+(k)=\tfrac{1}{2}\left(1+\frac{\omega}{\mu}\right)D_+(0)+\tfrac{1}{2}\left(1-\frac{\omega}{\mu}\right)D_-(0)+\frac{k^2}{4\pi^2}\int_\mu^\infty\frac{d\omega'}{k'}\left[\frac{\sigma_+(\omega')}{\omega'-\omega}+\frac{\sigma_-(\omega')}{\omega'+\omega}\right]+2\frac{f^2}{\mu^2}\frac{k^2}{\omega-\mu^2/2M}, \quad (12)$$

$$D_-(k)=\tfrac{1}{2}\left(1+\frac{\omega}{\mu}\right)D_-(0)+\tfrac{1}{2}\left(1-\frac{\omega}{\mu}\right)D_+(0)+\frac{k^2}{4\pi^2}\int_\mu^\infty\frac{d\omega'}{k'}\left[\frac{\sigma_-(\omega')}{\omega'-\omega}+\frac{\sigma_+(\omega')}{\omega'+\omega}\right]-2\frac{f^2}{\mu^2}\frac{k^2}{\omega+\mu^2/2M}, \quad (13)$$

where $D_\pm(k)$ is the real part of the forward scattering amplitude for $\pi^\pm$ with wave number $k$, mass $\mu$, and total energy $\omega$ (all quantities in the laboratory system), $\sigma_\pm(\omega)$ is the total interaction cross section at a total pion laboratory energy $\omega$, $f$ is the meson-nucleon coupling constant, and $M$ is the nucleon mass. The integrations over the singularities are carried out in the sense of Cauchy principal values. From these relations, using Orear's analysis of low-energy pion data[27] to obtain $D_\pm(0)$ and using Chew's analysis of pion-nucleon scattering data[5] to obtain $f$, Anderson, Davidon, and Kruse[28] have explicitly calculated the right hand sides of Eqs. (12) and (13) as functions of the pion laboratory energy from 0 to 300 Mev. The evaluation of the integrals requires knowledge of both positive and negative pion total cross sections at all energies, and hence the integrals contain implicitly the experimental errors in the determination of these cross sections.

In order to compare the results of this calculation with experiment, one may express the quantities $D_\pm(k)$ at a given energy in terms of the measured phase shifts at this energy. In particular, the quantity $D_+(k)$ is given by

$$(2k_b^2/k)D_+(k)=\sin2\alpha_3+2\sin2\alpha_{33}+\sin2\alpha_{31}+3\sin2\delta_{35}+2\sin2\delta_{33}+\cdots, \quad (14)$$

[27] J. Orear, Phys. Rev. **96**, 176 (1954).
[28] Anderson, Davidon, and Kruse, Phys. Rev. **100**, 339 (1955).

where $k_b$ is the pion wave number in the center-of-mass system. The experimental value of this quantity at 217 Mev is given in Table IV for the phase-shift solutions discussed above. The curve calculated by Anderson *et al.*[28] from Eq. (12) shows that the quantity $(2k_b^2/k)\times D_+(k)$ changes rapidly from positive to negative values at about 180 Mev, reaching a value of about $-1.88$ at 217 Mev. This result serves to exclude Solution III at our energy and is in agreement with the proposed resonant behavior of the phase shift $\alpha_{33}$. The errors associated with the results of the present experiment when $D$ waves are taken into account are large enough so as not to exclude agreement with the calculated curve.

## COULOMB INTERFERENCE

If one neglects the small Coulomb phase factors in Eqs. (4), (5), and (6) in comparison with unity, the differential scattering cross section may be written approximately as

$$\frac{t\sigma}{d\Omega}=\left(\frac{d\sigma}{d\Omega}\right)_{\text{Nuclear}}+\left(\frac{d\sigma}{d\Omega}\right)_{\text{Coulomb}}+\left(\frac{d\sigma}{d\Omega}\right)_{\text{Int}}^{(nf)}+\left(\frac{d\sigma}{d\Omega}\right)_{\text{Int}}^{(f)}, \quad (15)$$

where $(d\sigma/d\Omega)_{\text{Nuclear}}$ = differential cross section neglecting Coulomb forces, $(d\sigma/d\Omega)_{\text{Coulomb}}$ = differential cross section for Coulomb scattering only,

$$\left(\frac{d\sigma}{d\Omega}\right)_{\text{Int}}^{(nf)}=\frac{2}{k^2}\left(-\frac{n}{1-x}+a\right)\text{Re}\left[\frac{1}{2i}\left\{e_0+(2e_1^{+}+e_1^{-})x+(3e_2^{+}+2e_2^{-})\frac{3x^2-1}{2}\right\}\right], \quad (16)$$

$$\left(\frac{d\sigma}{d\Omega}\right)_{\text{Int}}^{(f)}=-\frac{2}{k^2}b(1+x)\,\text{Re}\left[\frac{1}{2i}\left\{(e_1^{+}-e_1^{-})+(e_2^{+}-e_2^{-})3x\right\}\right]. \quad (17)$$

At small angles where the dominant Coulomb term $-n/(1-x)$ becomes important and other Coulomb terms may be neglected, the sign of the term $(d\sigma/d\Omega)_{\text{Int}}^{(nf)}$ depends on the sign of the real part of the nuclear nonspin-flip scattering amplitude. Since both the dispersion relations discussed above and the hypothesis of a resonant behavior for the phase shift $\alpha_{33}$ predict that the real part of this amplitude should change sign in the vicinity of 180 Mev, a direct experimental measurement of this sign is of interest.

Pion-proton scattering experiments carried out by Orear[29] at 113 Mev and by Ferretti *et al.*[30] at 120 Mev indicate very strong preference for negative Coulomb interference, in agreement with the dispersion relations and with the generally accepted Fermi solution for the phase shifts. For the present experiment, the fairest way of determining the experimental preference for positive or negative Coulomb interference appears to be the following. The best fits to the data were found using the AVIDAC by varying all of the phase shifts involved, starting at points near the best fit values for the solutions considered. Since $e^w$ is a measure of the probability of the experimental results given a set of phase shifts and a path length, we take the ratio of this quantity for Solutions I, II, and III as a measure of the relative goodness of fit of these solutions to the data. The result is

$$e^{w(\text{I})}:e^{w(\text{II})}:e^{w(\text{III})}=1.49:1.49:1.0.$$

The preference for Solutions I and II, which correspond to positive Coulomb interference, over Solution III, which corresponds to negative Coulomb interference, is in agreement with the dispersion relations and with the resonance hypothesis. Solutions I and II, which differ only in the sign of $(d\sigma/d\Omega)_{\text{Int}}^{(f)}$, cannot be distinguished due to the smallness of the quantity $b$.

An alternate treatment of the problem of Coulomb interference is used by Orear[29] and by Ferretti *et al.*[30] These authors find the best fit set of phase shifts using only data from the region where Coulomb effects are negligible and then compare the fit in the Coulomb region between this set and the set with signs reversed. If one uses only scatterings of 40° or more, the best fit set of phase shifts found by the AVIDAC for Solution I is $\alpha_3=-20.2°$, $\alpha_{33}=115.2°$, and $\alpha_{31}=-7.3°$. The ratio of $e^w$ obtained for this solution to $e^w$ obtained for the solution with signs reversed, both solutions fitted to all the data, was 2.44.

A plot of the cross sections given by the AVIDAC for Solutions I and III is shown in Fig. 8. The solid line represents Solution I while the dashed line represents Solution III. The points represent a histogram of the experimental data. It should be pointed out that these points are not the representation of the data which the AVIDAC was instructed to fit but are simply shown as an indication of how good a fit to the data was obtained.

## CONCLUSION

In general, as long as $D$ waves and higher waves may be neglected in the analysis of $\pi^+$-proton scattering, and as long as Coulomb effects are not large, there are eight possible phase-shift solutions which may fit the data equally well. Four of these solutions correspond to a positive sign for the real part of the forward scattering amplitude at 217 Mev and are ruled out by the dispersion relations discussed above as well as by the preference of the data for positive Coulomb interference. Of the remaining four solutions, two have large values of $\alpha_3$ ($\alpha_3\doteq 76°$) and give relatively poorer fits to the

[29] J. Orear, Phys. Rev. **96**, 1417 (1954).
[30] Ferretti, Manaresi, Puppi, Quareni, and Ranzi, Nuovo cimento, **1**, No. 6, 1238 (1955).

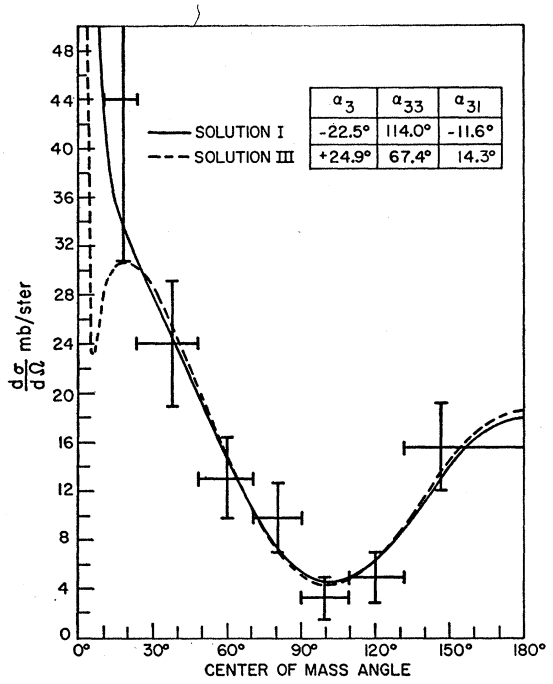


FIG. 8. Differential scattering cross section for 217-Mev $\pi^+$ mesons on protons.

data. In addition, these solutions seem unlikely in view of the value of $-20°$ for $\alpha_3$ measured by Glicksman and Anderson[11] at 165 Mev. The present experiment cannot distinguish between the remaining two solutions, i.e., Solution I, the Fermi solution, and Solution II, the Yang solution. However, as pointed out by Anderson *et al.*,[26] the rapid energy dependence of $\alpha_{31}$ required by the Yang solution at lower energies as well as the theoretical investigations of Chew and Low[5] make this solution less likely.

The general features of the Fermi solution found in the present experiment are in good agreement with the preferred solution of de Hoffman *et al.*[2] and with the features to be expected from a resonant behavior for $\alpha_{33}$. In addition to the results already discussed, the shift from backward to forward scattering, first observed at 189 Mev and very pronounced in the present experiment, is, in the absence of sizable $D$-wave phase shifts, very indicative of such a resonance. The sharp drop in the total $\pi^+$-proton cross section from its values measured between 170 Mev and 200 Mev is also in accord with such a resonant behavior. This sharp drop has been previously observed by Yuan and Lindenbaum[13] at Brookhaven, who give values for the total cross section at 214 Mev and 222 Mev in good agreement with our results.

## ACKNOWLEDGMENTS

The author is deeply indebted to the late Professor Enrico Fermi for his aid and encouragement throughout the early stages of this work. In the final stages, the active interest and assistance of Professor Herbert L. Anderson is also gratefully acknowledged. The author is also indebted to Dr. William C. Davidon, Dr. Arthur H. Rosenfeld, and Dr. Frank Solmitz for their valuable aid and advice, and to Jean Hall of the Argonne National Laboratory for making available the AVIDAC for computing the phase-shift solutions. Finally, we are indebted to the entire cyclotron staff, and in particular to Mr. Joseph Lack, Mr. Robert March, and Mr. John Lathrop for their efficient scanning.

## APPENDIX. ENERGY RESOLUTION

Because of the long range and large multiple scattering of high-energy pions, an analysis was made of the energy resolution of the counter arrangement used. According to Rossi and Greisen,[31] a parallel, monoenergetic beam of pions will, after passing through a thickness $dx$ of absorber, possess a Gaussian distribution of angles due to small angle multiple scattering with an rms angles given by

$$\langle\theta^2\rangle_{Av(dx)}=\frac{E_s^2}{p^2\beta^2}\frac{dx}{x_0}, \tag{A1}$$

where $E_s=21$ Mev and $x_0$ is the radiation length in the absorber. The rms angle as a function of depth in the absorber $\langle\theta^2(x)\rangle_{Av}$, was determined from Eq. (A1) by numerical integration. As long as the rms scattering angle as well as the individual scattering angles are small, this small-angle multiple scattering leads to a distribution in projected range with the following properties:

$$R-\langle R_x\rangle_{Av}=\tfrac{1}{2}\int_0^R\alpha(x)dx;$$
$$\langle R_x^2\rangle_{Av}-\langle R_x\rangle_{Av}^2=\tfrac{1}{2}\int_0^R dx\int_0^x ds\alpha^2(s), \tag{A2}$$

where $\alpha(x)=\int_0^x[d\langle\theta^2\rangle_{Av}/ds]ds$, $R$ is the true range along the meson path, and $R_x$ is the projection of $R$ on the incident beam direction. A numerical integration of Eq. (A2) gave for mesons of approximately 230 Mev, $R-\langle R_x\rangle_{Av}=3.44$ g/cm² of copper and $[\langle R_x^2\rangle_{Av}-\langle R_x\rangle_{Av}^2]^{\frac{1}{2}}=2.55$ g/cm² of copper. This distribution was then approximated by a Gaussian for the purpose of determining the energy spread of the incident beam.

In order to compare this result with the range curve obtained, one must also include the distribution in range due to statistical fluctuations in the number of ionizing collisions undergone by the mesons. The distribution in the distance traveled by a beam of high-velocity pions which decrease in energy from $E_1$ to $E_2$ by ionization loss is shown by Livingston and Bethe[32] to be approxi-

[31] B. Rossi and K. Greisen, Revs. Modern Phys. **13**, 263 (1941).
[32] M. S. Livingston and H. A. Bethe, Revs. Modern Phys. **9**, 245 (1937).

mately Gaussian with a mean square fluctuation given by

$$\langle (X-X_0)^2\rangle_{Av}=\int_{E_1}^{E_2}\frac{4\pi e^4NZ}{(dE/dx)^3}dE, \qquad \text{(A3)}$$

where $e$ is the electronic charge, $N$ is the number of atoms per cm$^3$ of absorber, $Z$ is the number of electrons per atom that are effective in the ionization process, and $-dE/dx$ is the rate of energy loss of the pion at the energy $E$. Using Eq. (A3) the rms spread in range due to this Gaussian straggling was calculated to be $[\langle (R-R_0)^2\rangle_{Av}]^{\frac{1}{2}}=1.54$ g/cm$^2$ of copper.

Taking into account the multiple scattering and straggling effects discussed above and assuming that the distribution in true range of the incident beam was approximately Gaussian, the rms spread in range was estimated from the rms spread observed in the counter range curve, which was $\pm 4.5$ g/cm$^2$ of copper. The mean range was taken to be the mean measured range plus the mean shortening due to multiple scattering. The resulting range of the incident beam was $124.4\pm 3.4$ g/cm$^2$ of copper. There was also an estimated uncertainty of about 1.5 g/cm$^2$ of copper in the value of the mean range.

PHYSICAL REVIEW VOLUME 101, NUMBER 3 FEBRUARY 1, 1956

# Disintegrations Produced in Nuclear Emulsions by 1.5-Bev Negative Pions*

R. D. HILL,† E. O. SALANT, AND M. WIDGOFF,‡ *Brookhaven National Laboratory, Upton, New York*, L. S. OSBORNE, A. PEVSNER AND D. M. RITSON, *Massachusetts Institute of Technology, Cambridge, Massachusetts*

AND

J. CRUSSARD§ AND W. D. WALKER,|| *University of Rochester, Rochester, New York*

(Received October 26, 1955)

The stars produced in nuclear emulsions by 1.5-Bev $\pi^-$ mesons are analyzed. The numbers of stars as a function of the numbers of prongs are obtained and compared with stars produced by protons of similar energies. The angular distributions of prongs from the pion-produced stars are also derived. An example of the decay of a hyperfragment $He^{6*}$ emerging from a pion star is described and the production of $K$ particles by 1.5-Bev pions is noted.

FOLLOWING the Brookhaven cloud-chamber experiments[1] in which hyperons and a $K$ particle were observed to be produced by 1.5-Bev pions, nuclear emulsions were exposed to high-energy negative pions from the Cosmotron. On account of the low intensity of pions ($\sim$1.5 per cm$^2$ per pulse) available at that time it was found necessary to irradiate the emulsions for a protracted period, and because of the high intensity of background radiation present it was found essential to have a clean pion beam and very good shielding of the emulsions. In the present experiment, stacks of 24 strips of 400$\mu$ G5 emulsions were irradiated in a 10-ton lead house at the end of a collimator 4 feet long. The total pion intensity in the emulsions was approximately 20 000 per cm$^2$. A preliminary report[2] of some of the results of scanning these emulsions has been given. Approximately 9 cc of emulsion in all were area-scanned by the three groups (B. N. L., M. I. T., and Rochester) analyzing these emulsions. Although a few $K$ particles were observed, these experiments were not fruitful in producing observable $K$-particle endings within the emulsions. The results of the experiments which will be given here include, in addition to the heavy mesons, information on pion-produced stars and several hyperfragments emitted from pion stars.

## PRONG DISTRIBUTIONS OF $\pi$-PRODUCED STARS

The population of $\pi$-produced stars in the emulsions can be gauged from the following details of area scanning by one group of observers. In 2.9 cc of emulsion (54.8 cm$^2$ of 400$\mu$ strips), 716 $\pi$-produced stars were observed, as compared with 740 neutron-produced stars.

In a sample of 75 $\pi$-produced stars, the numbers of stars as a function of the prong-number of the stars are given in Fig. 1. Also shown on the same plot and normalized to the same total number of stars, are distributions of prong numbers for 2.2-Bev protons[3] and 0.95-Bev protons.[4] It appears that the prong distribution for $\pi$-produced stars is not significantly different from that for proton stars; the 1.5-Bev $\pi$-produced star distribution lies approximately mid-

* Work performed under the auspices of the U. S. Atomic Energy Commission.

† Now at University of Illinois, Urbana, Illinois.

‡ Now at Harvard University, Cambridge, Massachusetts.

§ Now at Ecole Polytechnique, Paris, France.

|| Now at University of Wisconsin, Madison, Wisconsin.

[1] Fowler, Shutt, Thorndike, and Whittemore, Phys. Rev. **93**, 861 (1954).

[2] Hill, Salant, Widgoff, Osborne, Pevsner, Ritson, Crussard, and Walker, Phys. Rev. **94**, 797 (1954).

[3] Widgoff, Leavitt, Shapiro, Smith, and Swartz, Phys. Rev. **92**, 851 (1953).

[4] Lock, March, Muirhead, and Rosser, Proc. Roy. Soc. (London) **A230**, 215 (1955).